Geometrical influence on the strain distribution in biaxial composite specimens

E. Lamkanfi[1,1], W. Van Paepegem[1], J. Degrieck[1], A. Makris[2], C. Ramault[2] and D. Van Hemelrijck[2]

[1]*Department of Mechanical Construction and Production, Ghent University, Sint-Pietersnieuwstraat 41, B-9000 Ghent, Belgium.*

[2]*Department of Mechanics of Materials and Construction, Free University of Brussels, Pleinlaan 2, B-1050 Brussels, Belgium.*

ABSTRACT

In this paper, the influence of geometrical discontinuities on the strain distribution in cruciform specimen is investigated by use of a mixed experimental-numerical approach. For this purpose, the digital image correlation technique and the finite element method are employed to clarify the influence of these discontinuities on the failure mechanisms. It will be shown that anomalies such as the milled zone and the fillet corners which are introduced in the cruciform specimen to obtain a more uniform biaxial strain distribution result on the contrary in high strain concentrations. This observation is independent of the loading direction, i.e. whether the load is applied in a uni-axial or bi-axial way. Consequently, it will be proven that due to these anomalies in the specimen design, the specimen will fail prematurely due to onset of damage around these intensity zones. This complicates the assessment of bi-axial data for strength and failure criteria.

KEYWORDS: cruciform specimen, biaxial, radius, milled zone, discontinuous corners

1. INTRODUCTION

Composite materials are currently used, due to their high strength to weight ratio, in almost every demanding performance application. For a wider use of these materials, a better characterization should be obtained during real-life loading conditions. Therefore, uni-axial tests should be replaced by multi-axial or at least by bi-axial loading tests. This will provide a much better representation of the actual in-service loading conditions. Different techniques [1-6] can be found in the literature where geometries such as tubular or cruciform specimens are used. While the external applied loads are biaxial in the case of cruciform specimens, it remains a major task to obtain a multi-axial loading state in the material due to geometric discontinuities. In this paper the influence of the geometrical design on the strain distribution in cruciform specimens will be investigated in detail with the digital image correlation technique (DICT) and the finite element method (FEM). First the cruciform design will be discussed briefly. Also a brief overview will be given of the digital image correlation technique. This experimental technique will provide the strains on the surface of the specimen. In addition to these tests, the 2D and the 3D finite element models will be discussed. Also the impact of the loading direction on the strain distribution will be presented. Finally some conclusions will be drawn which will point out the importance of cruciform design in the research for biaxial strength and failure criteria.

[1] Author to whom correspondence should be addressed : ebrahim.lamkanfi@ugent.be

2. CRUCIFORM DESIGN

2.1 Cruciform specimen

During the last decades, several researchers [7-15] have tried to perform biaxial tests on different kinds of composite materials. One of the first geometrical types that were used to obtain a bi-directional stress state were tubular specimens. The reason why other geometries than this tubular ones had to be investigated was mainly due to the fact that the use of internal pressure, in combination with axial or torsional forces, resulted in a high built-up of stresses through the thickness direction. The impact of these stresses on the global stress state was relatively high, which indicated that these tubular geometries could only be used in tubular-like applications such as pressure vessels. Therefore, it was believed that in other applications where the thickness stresses were small, cruciform specimens could give a better insight in the true material behaviour. Besides a wide range of loading systems, also a variety of cruciform geometries have been developed with the most important requirement that the load had to be transferred in a proper way to the biaxial zone of the specimen.

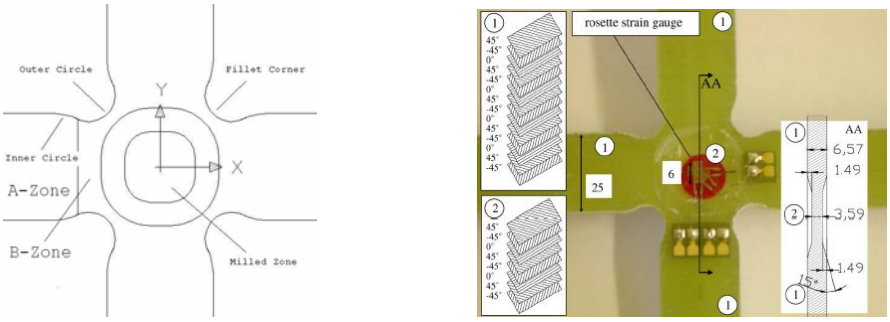

Figure 1. Cruciform geometry (a) and the used stacking sequence together (b).

The cruciform specimen discussed in this paper (Fig. 1a) is a glass fibre reinforced plastic (GFRP), manufactured by LM Glasfiber (Denmark) using the RTM technology. This composite, which is widely used in the wind turbine industry for the construction of rotor blades, has a $[(\pm 45/0)_4/\pm 45]$ stacking sequence (Fig. 1b). The [±45] plies contain a non-woven glass roving in two layers with one layer in +45° and one layer in -45°. Since the [±45] plies are considered as internally symmetric, a symmetric configuration is obtained. In the center of the laminate, one group of [±45/0] at each side of the specimen is milled away. This gradual thickness reduction, with an angle of 15° with the horizontal (Fig. 1b), has been introduced in the material because of the greater capacity of the center zone to withstand a larger stress compared with that of the arms. No milling-out will lead therefore to breakage in the arms. A second discontinuity can be found in the corners where two rounding radii have been used to cut-out the arms in that region: an inner radius of 25 mm and an outer radius, nearer to the centre, of 12.5 mm (Fig. 1a). These cut-outs have to direct the loads from the horizontal arms to the vertical ones.

2.2 Digital image correlation technique

Due to the complex specimen geometry, the relation between the externally applied loads in the arms of the cruciform specimen and the resulting stress field in the center of the specimen cannot be determined analytically. The use of strain gages or an extensometer is not sufficient because of the average value of the deformation along their gage length. And because of the

fact that it is very difficult to realize a uniform stress and strain distribution in the biaxially loaded centre, the strain field is experimentally measured with the Digital Image Correlation Technique (DICT) [16]. The principle behind this technique is based on a comparison of images taken at different loading steps. First a random speckle pattern is applied onto the surface of the cruciform. Then a Charge Couple device (CCD) camera acquires images from the area of interest on the surface of the specimen in the un-deformed and deformed states. In our experiments two cameras were used (Fig. 2) to measure both the in-plane and the out of plane displacements in the zone where the surface is milled out. The obtained high resolution images are correlated to determine the deformations by tracking the specific movement of these greyscale patterns relative to their original positions. Finally some advanced mathematical procedures are applied to these deformations to calculate the surface strains.

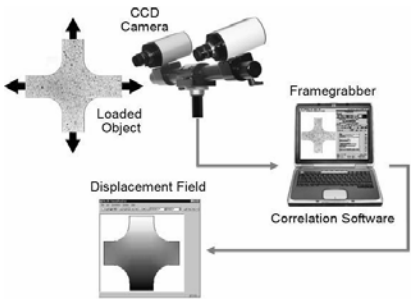

Figure 2. The principle behind the digital image correlation technique

In Fig. 3, one can see an example obtained with this optical technique where 80% of the ultimate load F_x/F_y=46.2kN/12kN, i.e. 36.9kN/9.6kN, is applied. In the following paragraph the finite element method will be used to reproduce these strains. This will make it possible to compare the strain fields on the surface of the cruciform specimen obtained by the digital image correlation technique and the calculated linear elastic strain fields.

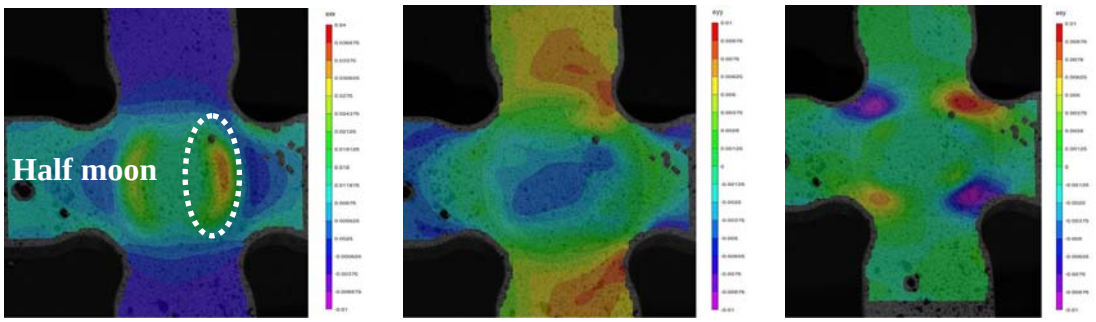

Fig. 3 : Strains ε_{xx} (a) , ε_{yy} (b) and ε_{xy} (c) along of a biaxial loaded specimen obtained with the DICT. Biaxial load at 80% of the ultimate load.

3. FINITE ELEMENT MODEL

This method will be used here as a detailed technique to study the strain distribution of the cruciform specimen. Besides the implementation of a shell model, also a more complex three dimensional model has been developed to investigate the influence of geometrical discontinuities on the strain distribution. In both the models the same geometry, stacking sequence, boundary conditions and material characteristics have been used. Whereas for the

3D model all the material characteristics from Table 1 are employed, the 2D case uses the homogenized elastic properties for the composite laminate which are derived by means of Classical Lamination Theory. In this way only the in-plane stress and strain components can be obtained in the two dimensional model.

TABLE 1: Material characteristics for glass fibre reinforced epoxy.

Young modulus [N/mm^2]			Poisson ratio [-]			Shear modulus [N/mm^2]		
E_1	E_2	E_3	ν_{12}	ν_{13}	ν_{23}	G_{12}	G_{13}	G_{23}
39100	14440	14440	0.294	0.294	0.294	5390	5390	5390

3.1 Two-dimensional model

Before discussing the 3D model, an attempt will be made to reproduce the DIC images from Fig. 3 by using a 2D finite element model. For this purpose, two dimensional S4R shell elements with 4 degrees of freedom and with the reduced integration scheme have been used. The results can be found in Fig. 4a, Fig. 4b and Fig. 4c where the strains ε_{xx}, ε_{yy} and γ_{xy} are shown in the global coordinate system. These strains can be compared with those in Fig. 3. One can clearly see that the strains ε_{yy} (Fig. 4b) and $\gamma_{xy}/2$ (Fig. 4c) match very well with the corresponding ones in Fig. 3b and Fig. 3c. This is not the case for the ε_{xx} in Fig. 3a and Fig. 4a. The three dimensional model has to clarify this mismatch.

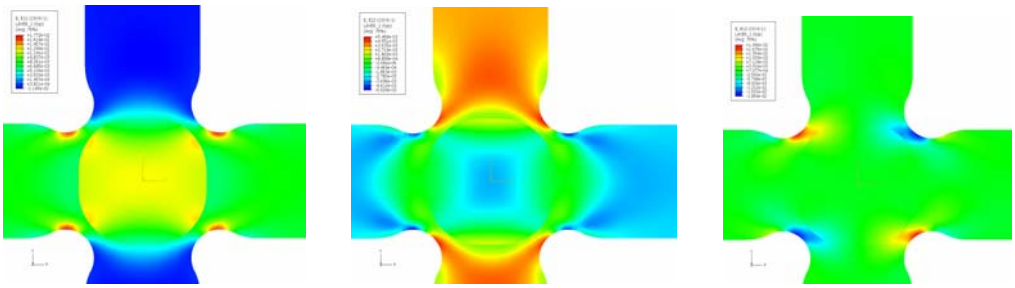

Fig. 4: Strains ε_{xx} (a), ε_{yy} (b) and γ_{xy} (c) in the global coordinate system for the 2D model. Biaxial applied load is taken at 80% of the ultimate load.

3.2. Three-dimensional model

In this detailed 3D model, each layer is modelled independently from the others. For the type of elements, 8 node brick continuum elements with the reduced integration scheme have been chosen. In Fig. 5a, Fig. 5b and Fig. 5c, the strains ε_{xx}, ε_{yy} and γ_{xy} are depicted. A comparison with the DIC images in Fig. 3 and the 2D results in Fig. 4 shows that the surface strains ε_{yy} and $\gamma_{xy}/2$ correspond also here very well. However, the ε_{xx} strains remain much higher than those found in the DIC Fig. 3a. This is particularly the case at the interface between the flat surface of the milled zone and the skew edges, where a half moon pattern is visible. Despite of the fact that the same pattern is captured by the 3D model and the DIC experiment, these

ε_{xx} values remain higher (3.3%) in this area for the DIC method compared with those found in the 3D model (1.318%). It is the authors' belief that this half moons pattern is due to the milling out of the centre zone and therefore a result of the discontinuity in the cruciform geometry.

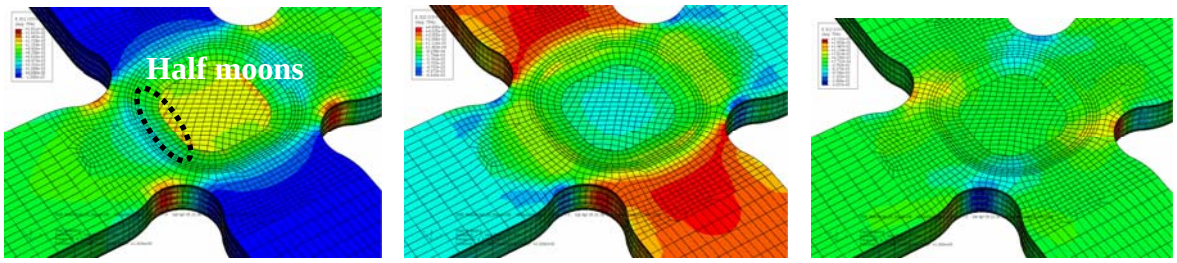

Fig. 5 : Strains ε_{xx} (a), ε_{yy} (b) and ε_{xy} (c) in the global coordinate system for the 3D model.

5. GEOMETRICAL DISCONTINUITIES

5.1 Milled Area

In this paragraph the influence of the load direction on the half moon pattern, shown in Fig. 5a and Fig. 3a, will be investigated. For this purpose, two models are presented where the loads are applied in a uni-axial way: one in the x-direction and the other in the y-direction. Hereby, the same load ratio (F_x/F_y = 3.85/1) is used as the one above. In the Fig. 6a and Fig. 6b it can be seen that the half moon pattern occurs in both models. A similar pattern is also visible for the inter-laminar strains ε_{xz} and ε_{yz}, respectively shown in Fig. 7a and 7b. These high strain intensities at the interface of the milled zone and the skew edges clearly indicate that the surface discontinuity is responsible for the existence of the half moons and that cracks will be initiated at these places, as shown in the experiment of Fig. 8.

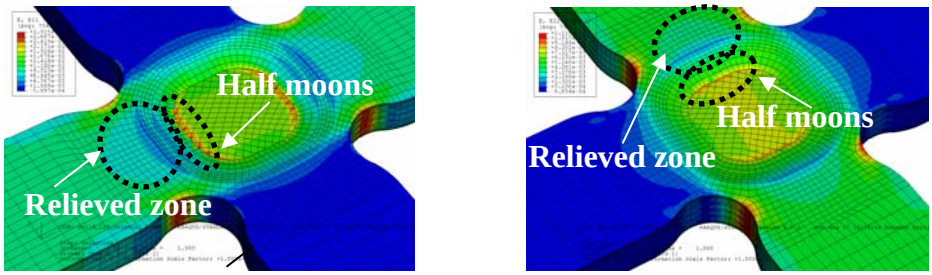

Fig. 6 : Half moon pattern in x-direction (a) and y-direction (b) loaded specimen

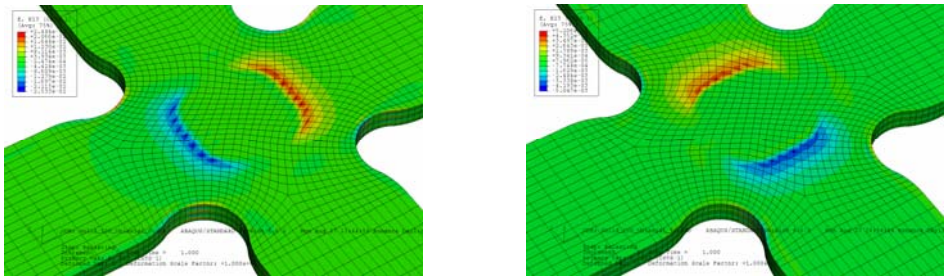

Fig. 7 : Strains ε_{xz} due to x-direction loading (a) and strains ε_{yz} due to y-direction loading (b). Hereby the three top and bottom layers are disguised.

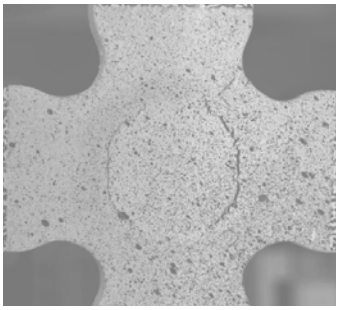

Fig. 8 : Crack at the transition between the skew edges and the flat zone of the milled area.

5.2 Strain relieved zone and rounding radii

In all of the simulations above, the presence of a relief zone can be found in the direction of the highest load. It is also interesting to notice that these areas are located just at the transition of the two rounding radii, which have to lead the loads into the central area. It appears that just the contrary happens. This can be clearly seen on the 2D (Fig. 9a) as well as on the 3D model (Fig. 9b), where high strain concentrations are visible in the fillet corners. Moreover, a detailed study of the cross section of the arms in the neighbourhood of these corners, shows the formation of a bulged (Fig. 10a) and a contracted (Fig. 10b) zone. This change in cross section deformation happens at the transition between the inner circle and the outer circle (Fig. 1a). This could be the reason why the rounding radii disturb the incoming load resulting in the high strain zones. It is also shown in Fig. 11a and Fig. 11b that the orientation of the fibres has no influence on this bulging-contraction phenomenon. Even in the case of an isotropic material (Fig. 12a and Fig. 12b), this effect remains. Therefore, it can be concluded that the corner radii are responsible for the strain concentrations in their vicinity.

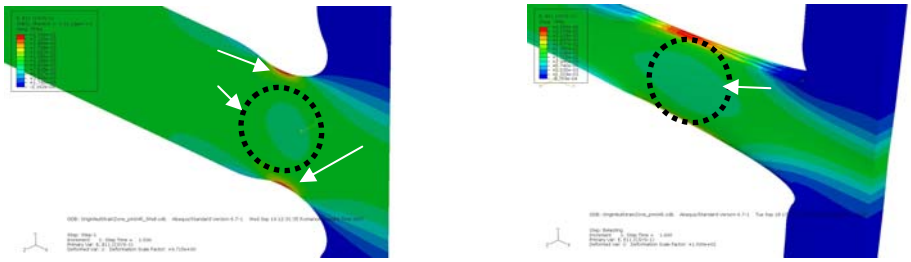

Fig. 9 : Relieved area in between the two corner radii : the two-dimensional case (a) and the three-dimensional model (b).

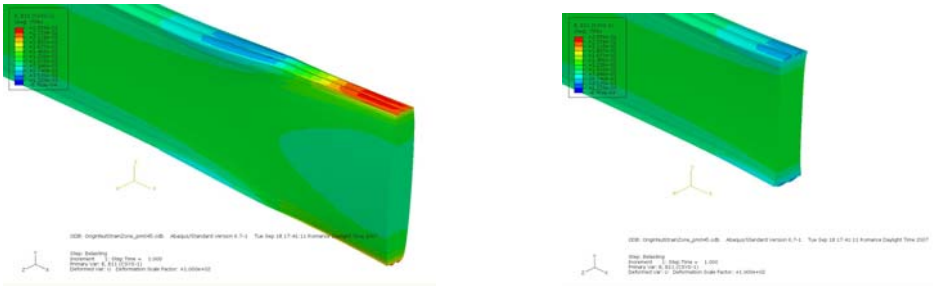

Fig. 10 : Strains ε_{xx} in $[\pm 45^{\circ}/0^{\circ}]$ lay-up model without milled layers at the inner (a) and the outer (b) rounding circle in a x-direction loading case. Bulging (a) and contraction (b) effect is respectively shown.

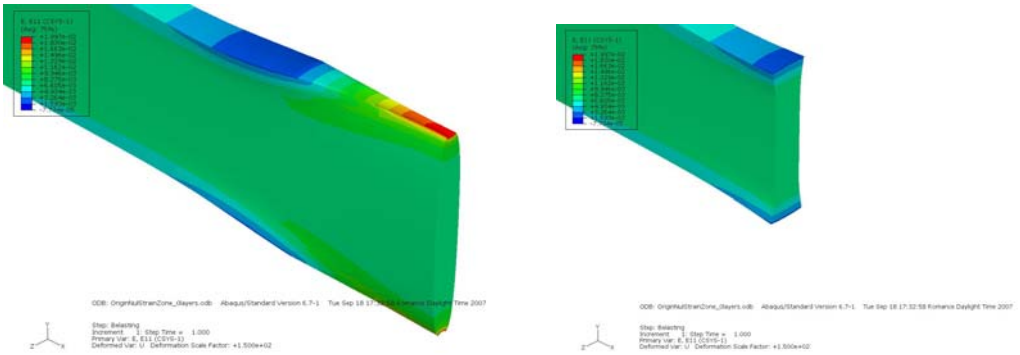

Fig. 11 : Strains ε_{xx} in a pure $[0^{\circ}]$ lay-up model without milled layers at the inner (a) and the outer (b) rounding circle. Bulging (a) and contraction (b) effect is respectively shown.

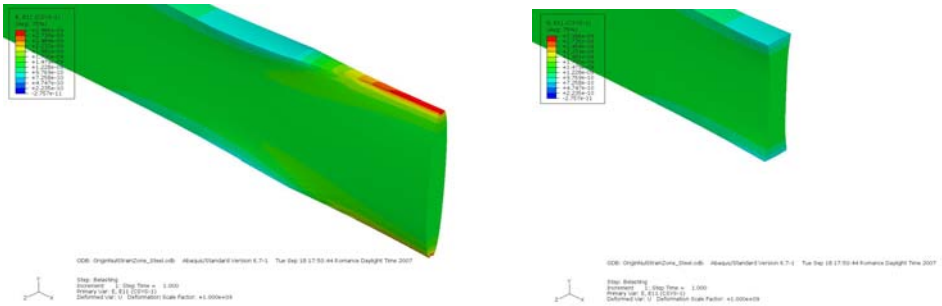

Fig. 12 : Strains ε_{xx} in homogeneous, isotropic (steel) model without milled layers at the inner (a) and the outer (b) rounding circle. Bulging (a) and contraction (b) effect is respectively shown.

6. CONCLUSIONS

Discontinuities such as the milled zone and the fillet corners which are introduced in the cruciform specimen to obtain a more uniform biaxial strain distribution, result on the contrary in high strain concentrations under any kind of load (uni-axial or biaxial) and independent of the load direction. The development of high strain intensity zones lead to cracks at the edge of these milled surfaces. Also the high strains in the loading arm at the fillet corner are due to a discontinuity in the corner geometry. Here the transition from the inner circle to the outer circle results in a contraction zone and bulging zone. Both effects complicate the assessment of the ultimate biaxial strength due to onset of damage around the high strain intensity zones. Therefore, a premature failure is induced before reaching the ultimate strength in the biaxial milled zone.

ACKNOWLEDGMENTS

The authors gratefully acknowledge the support for this research by the Fund for Scientific Research - Flanders (FWO).

REFERENCES

1. Zouani, T. Bui-Quoc and M. Bernard, “Cyclic stress-strain data analysis under biaxial tensile stress state”, Experimental mechanics, 39(2), 92-102, 1999.

2. D. Lefebvre, C. Chebl, L. Thibodeau and E. Khazzari, “A high-strain biaxial testing rig for thin-walled tubes under axial load and pressure”, Experimental mechanics, 23(4), 384-392, 1983.
3. J.P. Boehler, S. Demmerle and S. Koss, “A new direct biaxial testing machine for anisotropic materials”, Experimental mechanics, 34(1), 1-9, 1994.
4. J.S. Welsh and D.F. Adams, “Development of an electromechanical triaxial test facility for composite materials”, Experimental mechanics, 40(3), 312-320, 2000.
5. E. Shiratori and K. Ikegami, A new biaxial tensile testing machine with flat specimen, Bul. Tokyo Inst. Of Tech., 82, 105-118, 1967.
6. Y. Yu, M. Wan, X.D. Wu and X.B. Zhou, “Design of a cruciform biaxial tensile specimen for limit strain analysis by FEM”, Journal of Materials Processing Technology, 123(1), 67-70, 2002.
7. Atcholi EK, Oytana C, Superposed tension-flexure of composite materials : experimental method and example of application, *Composites*, vol 23, 327-333, 1992
8. McDiamir DL, A new analysis of fatigue under combined bending and twisting, *Aeronautical Journal*, 325-329, 1974
9. Kakuno H, Kawada Y, A new criterion of fatigue strength of a round bar subjected to combined static and repeated bending and tension, *Fatigue of Engineering Materials and Strcutures*, vol 2 (2), 229-236, 1979
10. Hong N, Xin Q, Weixiun F, A criterion for fatigue damage under combined bending and torsion based on the local stress-strain mathod, *Fatigue & fracture of engineering materials & structures*, vol 15 (2), 225-227, 1992
11. Ferry L, Gabory D, Sicot N, Berard JY, Perreux D, Varchon D, Experimental study of glass-epoxy composite bars loaded in combined bending and torsion loads : Fatigue and characterisation of the damage growth, *International Conference on fatigue of composites*, 266-273, 1997
12. Ferry L, Perreux D, Varchon D, Sicot N, Fatigue behaviour of composite bars subjected to bending and torsion, *Composites Science and Technology*, vol 59, 575-582, 1999
13. Zouani A., Bui-Quoc T., Bernard M., A proposed device for biaxial tensile fatigue testing, Fatigue and Fracture-1996, ASME PVP-323, vol. 1, p. 331-339, 1996
14. Hazell C.R., Marin J., A possible specimen for the study of biaxial yielding of materials, Int. J. Mech. Sci., vol. 9, p. 57-63, 1967
15. Bird J.E., Duncan J.L., Strain hardening at high strain in aluminium alloys and its effects on strain localisation, Met. Trans., vol. 12A, p. 235-241, 1981
16. J.-N. Perie, S. Calloch, C. Cluzel, and F. Hild, “Analysis of a Multiaxial Test on a C/C Composite by Using Digital Image Correlation and a Damage Model”, Experimental Mechanics, 42(3), 318-328, 2002